2020年4月 矿 床 地 质 第39卷 第2期
April, 2020 MINERAL DEPOSITS 39(2): 256~272

文章编号: 0258-7106(2020)02-0256-17 Doi: 10.16111/j.0258-7106.2020.02.004

矽卡岩型钨矿床成矿作用研究进展*

李佳黛[1,2,3],李晓峰[1,2,3]

(1 中国科学院矿产资源研究重点实验室,中国科学院地质与地球物理研究所,北京 100029; 2 中国科学院地球科学研究院,北京 100029; 3 中国科学院大学地球与行星科学学院,北京 100049)

摘 要 钨具有极高的熔点和硬度,是现代生活、工业、国防和高科技领域中不可或缺的基础材料。研究显示,矽卡岩型钨矿是世界钨矿床中最主要的类型,广泛分布于受俯冲影响的环太平洋大陆边缘和与碰撞有关的欧亚大陆内部古大陆边缘,形成时代集中在中生代和古生代。钨在岩浆演化过程中呈现不相容的特征,因此与钨矿化相关的岩浆岩演化程度较高,包括S型、A型以及高分异I型花岗岩。钨具有较高的流体亲和性,使其在熔-流体分异过程中倾向于富集在共存的流体相。钨在热液流体中以氯化物、氟化物和碳酸盐络合物,以及同多钨酸盐和杂多钨酸盐等形式迁移,主要受源岩、围岩成分和流体物化条件等因素影响。矽卡岩型钨矿的成矿作用存在多期次、多阶段演化特征,不同阶段的成矿流体的温度和盐度存在差异。白钨矿是矽卡岩型钨矿中主要的矿石矿物,其沉淀可能受到多种机制的影响,如降温、流体混合、流体沸腾及流体-围岩反应等。文章简要综述了世界矽卡岩型钨矿的时空分布、地质特征和相关成因矿物学研究,并重点总结了钨的成矿岩浆-热液体系特征,钨在岩浆-热液演化过程中的地球化学行为及其迁移和沉淀机制等方面的研究成果。文章指出,为了完善矽卡岩型钨矿的成矿和找矿勘查模型,应当加强矽卡岩型钨矿的成矿时代、成矿物质和流体来源以及成矿环境的精细研究。

关键词 地质学;成矿作用;迁移和沉淀机制;矿物学;矽卡岩型钨矿

中图分类号:P618.67 **文献标志码**:A

Research progress in metallogenesis of skarn-type tungsten deposits

LI JiaDai[1,2,3] and LI XiaoFeng[1,2,3]

(1 Key Laboratory of Mineral Resources, Institute of Geology and Geophysics, Chinese Academy of Sciences, Beijing 100029, China; 2 Innovation Academy for Earth Science, Chinese Academy of Sciences, Beijing 100029, China; 3 College of Earth and Planetary Sciences, University of Chinese Academy of Sciences, Beijing 100049, China)

Abstract

Tungsten, as a relatively rare metal with high melting point and hardness, has been found necessary in modern life, industry, national defense, and high-tech fields. Studies have shown that world's tungsten deposits are dominated by skarn-type tungsten deposits, which are widely distributed in the subduction-type plate boundary along the Pacific Ocean and the collision-type plate boundary in the Eurasia continent. The significant development of tungsten skarn in geological history mainly occurred in the Mesozoic and Paleozoic period. Tungsten is incompatible in the evolution of magma, and hence the magmatic rocks associated with tungsten mineralization are S-type, A-type or highly differentiated I-type. The high fluid affinity caused preferential enrichment of tungsten in the coexisting fluid phase during melt differentiation. Tungsten could be transported by various complexes in hydrothermal fluids, including chloride, fluoride and carbonate complexes, as well as homopolytungstate and heteropolytungstate, mainly depending on source/host-rock composition and physicochemical conditions. The

* 本文得到国家自然科学基金项目(编号:41472080)资助

第一作者简介 李佳黛,女,1993年生,博士研究生,矿物学、岩石学、矿床学专业。Email: ljd3737@163.com

收稿日期 2019-09-28;改回日期 2020-03-01。秦思婷编辑。

ore-forming processes of skarn-type deposit generally included multiple stages, which displayed obvious distinctions in the temperatures and salinities of mineralizing fluids. Scheelite is the main ore mineral in skarn-type tungsten deposits, and its deposition might have been controlled by various mechanisms, such as cooling, fluid mixing, fluid boiling, and fluid-rock interaction. This paper made a brief review of spatial and temporal distribution, ore deposit geology, and mineralogy of tungsten deposits studied before, and mainly focused on the geochemical behavior in the processes of magmatic-hydrothermal evolution and mechanisms of transport and deposition of tungsten. It is held that researches should be further strengthened in such aspects as the duration and evolution of tungsten skarn systems, the origin of tungsten, and the physical and chemical conditions of tungsten precipitation.

Key words: geology, metallogenesis, mechanisms of transport and deposition, mineralogy, skarn-type tungsten deposits

钨(W)是一种极为重要的稀有难熔金属,广泛应用于现代生活、电子工业、汽车工业、航空航天和原子能等领域。世界钨储量大约3.1 Mt,中国的钨储量约占61.3%(Sheng et al., 2015)。根据成矿作用性质、成矿物质来源等因素,世界钨矿床可划分为岩浆成因、沉积成因、(火山)沉积-变质改造成因和现代表生成因4种类型(康永孚等,1991;石洪召等,2009)。具体地,结合成矿机制、成矿地质特征及矿物组合特征将岩浆成因矿床进一步划分为矽卡岩型、石英脉型、斑岩型、云英岩型、花岗岩型和火山岩型(夏庆霖等,2018)。其中,矽卡岩型白钨矿矿床是最主要的类型,分别约占世界和中国总储量的50%和39.32%(Sheng et al., 2015)。狭义的矽卡岩型钨矿多呈透镜状、层状-似层状或囊状产出于中酸性花岗岩及花岗质混合岩和碳酸盐类及其他含钙质岩石接触带及附近,主要通过接触双交代和渗滤交代作用形成(林运淮,1982;毕承思,1987)。但研究表明,薄层灰岩或者不纯的碳酸盐类岩石和与其物理化学性质有明显差异的岩石(如泥岩、火山岩、页岩等)互层时,同样有利于矽卡岩型矿化(多受断裂构造控制)的富集(Kwak et al., 1981)。因此,广义的矽卡岩型钨矿主要是通过不纯碳酸盐岩的变质重结晶作用、不同岩性岩石之间的接触双交代作用以及岩浆热液、混合岩化热液和变质热液的渗滤交代作用形成的,无论是中酸性岩体还是碳酸盐等含钙质岩石均不是必要条件(Meinert et al., 2005)。前人根据矽卡岩矿物组合(Fe^{2+}和Fe^{3+}的相对含量)、围岩组成(碳质和赤铁矿的相对含量)以及相应成矿深度(变质温度和氧化地下水的参与情况)将矽卡岩型钨矿大致划分为氧化型(W-Mo-Cu)和还原型(W-Sn-F)(Newberry et al., 1981; Meinert et al., 2005)。但大部分矽卡岩型钨矿具有多种蚀变矿化的叠加,可能同时存在还原型和氧化型矿化(如柿竹园钨矿),因此,简单地划分为这2种类型还不够全面。近年来,随着实验分析技术和矿产勘查方法的发展与进步,使得典型矿床成因的深度剖析成为可能,并且相继发现了一些新的大中型矽卡岩型钨矿,如华南的朱溪钨铜矿(约149 Ma,Song et al., 2018)和魏家钨矿(159~158 Ma, Zhao et al., 2016),以及加里东期的社洞钨钼矿(陈懋弘等,2011)。因此,全面深入地理解和认识矽卡岩型钨矿的特征和成矿规律十分必要。本文在简要介绍国内外矽卡岩型钨矿的时空分布、地质特征和相关矿物学研究的基础上,系统归纳了钨的成矿岩浆-热液体系特征,钨在岩浆-热液演化过程中的地球化学行为及其迁移和沉淀机制等方面的研究成果。从成矿物质的来源、迁移形式和沉淀机制3个方面总结了矽卡岩型钨矿的成矿作用特点,有助于指导找矿工作。

1　矽卡岩型钨矿的时空分布

全球钨矿床主要分布在受俯冲作用影响的广义环太平洋大陆边缘,其次分布于广义欧亚大陆内部古大陆边缘碰撞带(图1)(徐克勤等,1987)。中国钨矿床多数分布在造山带中,集中在南岭成矿带,同时,秦岭-祁连山-昆仑山成矿带、东秦岭成矿带、三江成矿带、天山-北山成矿带以及内蒙古-大兴安岭成矿带也是重要的钨矿床分布区(图2)。全球范围内,钨矿床从太古代到第四纪都有产出,但是主要集中在古生代和中生代,其次为新生代。其中,矽卡岩型钨矿基本发育于中生代和古生代,前寒武纪也有少量发育。类似地,中国钨矿床的成矿时代也从元古代跨度到喜马拉雅期,燕山期为最主要的成矿期(表1),超过全国总储量的84%,其中,矽卡岩型钨矿主

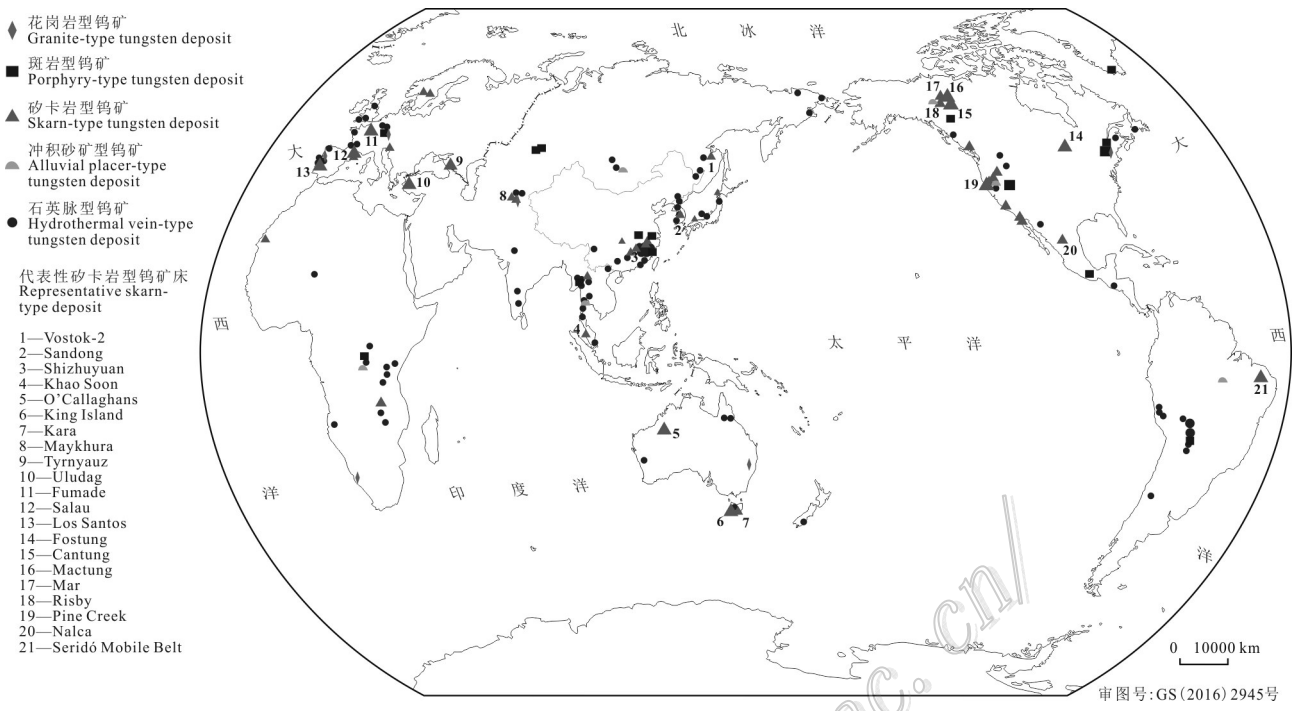

图1 世界主要钨矿床分布图(据Brown et al., 2014; Sheng et al., 2015修改)

Fig. 1 Distribution of world's major tungsten deposits (modified after Brown et al., 2014; Sheng et al., 2015)

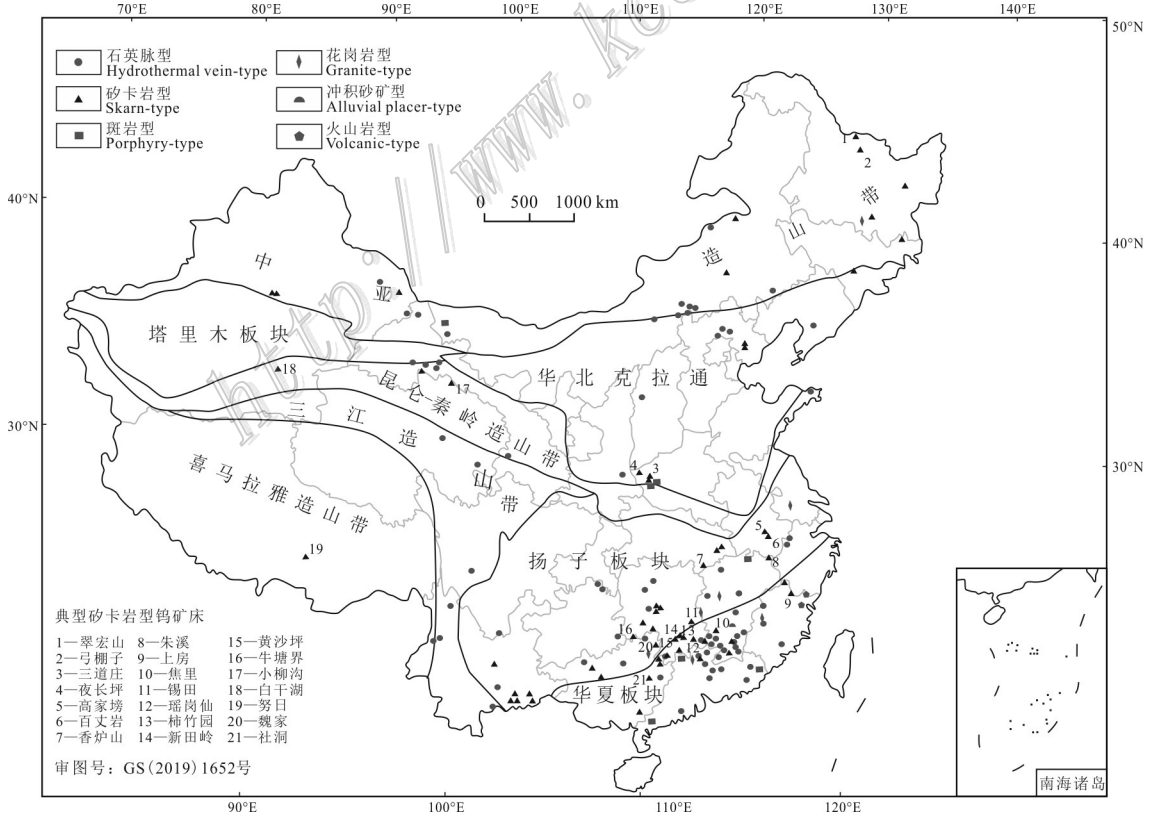

图2 中国主要钨矿分布图(据Sheng et al., 2015修改)

Fig. 2 Distribution of major tungsten deposits in China (modified after Sheng et al., 2015)

要发育在燕山期,加里东期—海西期和喜马拉雅期也见少量发育(Sheng et al., 2015)。国内外著名的大型-超大型矽卡岩型钨矿(表1)包括加拿大Mactung(储量33 Mt,品位0.88%)和Cantung(储量4.2 Mt,品位1.6%),美国Pine Creek(>6 Mt),朝鲜Sangdong(储量9.52 Mt,品位0.56%),澳大利亚King Island(储量6.58 Mt,品位0.64%~0.8%),土耳其Uludag以及中国朱溪(储量3.44 Mt,品位0.54%)、香炉山(储量约0.22 Mt,品位0.641%)、柿竹园(储量0.8 Mt,品位0.35%)、新田岭(储量0.3 Mt,品位0.37%)和瑶岗仙(储量0.236 Mt,品位1.27%)矿床。

2　矽卡岩型钨矿的地质特征

全球范围内,与矽卡岩型钨矿相关的地层围岩为元古界—古近系含碳酸盐或含钙质的岩石,以不纯灰岩(如泥岩-碳酸盐混合/互层的层序)更为有利。国外的矽卡岩型钨矿多与具有大范围高温变质晕的粗粒、等粒状中酸性-酸性岩基(多见伟晶岩和细晶岩岩脉发育其间)有关,包括晚古生代—晚白垩世花岗闪长岩-石英二长岩;而中国矽卡岩型钨矿的成矿岩体侵位相对较浅,以中细粒结构为主,似斑状结构次之,主要包括早古生代和中晚侏罗世—早白垩世黑云母花岗岩、二长花岗岩、花岗斑岩以及少量花岗闪长岩(表1)。白钨矿为最主要的金属矿物,呈浸染状颗粒或裂隙填充物产出,多伴生其他金属矿化(以Cu、Mo、Sn、Zn和Bi为主)。具有开采价值的矽卡岩型钨矿品位为0.1%~1.5%,矿床储量范围大致10^4~10^7 t,高品位钨矿石与含水矿物和退蚀变作用关系密切(Meinert et al., 2005; Brown et al., 2014)。矿体形态复杂,主要受接触带控制呈层状、似层状、透镜状,或受断裂、裂隙控制呈脉状、带状、扁豆状、囊状(毕承思,1987)。根据原岩成分和矽卡岩矿物组合可以分为由富Ca、Fe、Al的硅酸盐矿物(如钙铁铝榴石、钙铁辉石、硅灰石、符山石、绿帘石)组成的钙质钨矽卡岩,以及由富Mg、Ca的硅酸盐矿物(如镁橄榄石、尖晶石、蛇纹石、金云母、透辉石)组成的镁质钨矽卡岩。由于白云质岩石不利于含钨矽卡岩以致镁质钨矽卡岩的形成,国外大部分矽卡岩型钨矿中的含矿矽卡岩为钙质矽卡岩。但近年来的研究发现,国内镁质矽卡岩具有形成钨矿的潜力,如江西朱溪钨铜矿和湖南魏家钨矿,其镁质钨矽卡岩主要形成于晚侏罗世花岗质岩体(朱溪,约150 Ma黑云母二长花岗岩;魏家,约158 Ma花岗斑岩)与白云岩接触带(朱溪,中石炭统黄龙组;魏家,中泥盆统棋梓桥组),均发育大量萤石,表明富F流体有利于镁质矽卡岩以及白钨矿的形成(Song et al., 2018)。由于侵入岩体和成矿作用的多期性以及赋矿地层的岩性分带,大型矽卡岩型钨矿多存在不同类型的蚀变矿化相互叠加。如柿竹园矿床在钙质矽卡岩型W(白钨矿)-Sn-Mo-Bi矿化结束后,叠加形成云英岩型W(黑钨矿)-Mo-Bi-Sn-Be矿化,并伴随晚期花岗斑岩的侵入形成镁质矽卡岩型Pb-Zn-Ag矿化(林运淮,1982;Chen et al., 2016);Mactung矿床在泥质地层单元中发育云英岩型W(白钨矿)-Mo矿化,在灰岩单元则形成矽卡岩型W(白钨矿)矿化(Selby et al., 2003)。矽卡岩型钨矿形成阶段大致可依据经典的"三期五阶段"划分为矽卡岩期(早期矽卡岩阶段和晚期矽卡岩阶段)、氧化物期(石英-白钨矿阶段)和硫化物期(早期石英-硫化物阶段和晚期石英-硫化物阶段)(毕承思,1987),但具体划分因各矿床的地质特征而异,尤其需要注意退蚀变阶段的细分和不同蚀变矿化类型与矿化阶段的对应关系。

3　钨的成矿岩浆系统

上地壳钨的平均含量为1.9×10^{-6}(Rudnick et al., 2003),并且钨在岩浆演化过程中呈现不同程度的不相容性(Linnen et al., 2005; Breiter et al., 2007)。因此,与钨矿化具有成因联系的岩浆岩多形成于岩浆演化的晚期阶段(Newberry et al., 1986),主要为I/S分异型和A型花岗岩(图3d),其成因上主要来源于变质的沉积物基底或变质的火成岩基底±地幔分异物质或新生地壳的部分熔融(Breiter, 2012; Romer et al., 2016)。前人曾对比指出,中国与(高分异)I型花岗岩有关的钨矿床以中小型为主,主要的大中型矿床还是与S型花岗岩有关;而世界其他范围,如北美、日本、韩国等地区的巨型矽卡岩型白钨矿矿床大多数则与(高分异)I型/I-S混合型花岗岩有关(Newberry et al., 1986; 毕承思,1987)。由于与钨矿化相关的岩浆岩具有不同的成因类型,因此,对应的钨成矿花岗岩也具有不同的地化成分以及演化特征。但总体上,钨成矿花岗岩$w(SiO_2)$较高,多数集中在75%左右,$w(Na_2O+K_2O)$较高,大部分大于7%,具有高硅富碱的特征。其中,矽卡岩型和石英脉型钨矿的成矿岩体碱质含量变化范围较大,从钙碱性到碱

表1 全球代表性矽卡岩型钨矿床的分布、成矿时代和岩体特征

Table 1 The distribution, mineralization ages, and characteristics of magmatic rocks of representative tungsten deposits worldwide

矿床	矿床类型和矿化元素	国家或地区	储量及品位	成矿岩体	成矿时代/Ma	资料来源
朱溪	矽卡岩W-Cu	江西	$w(WO_3)$3 440 000 t, 0.54%	黑云母二长花岗岩、花岗(斑)岩	Ar-Ar (150.6±1.5)、(150.04±0.94)；Re-Os (145.1±1.5)；榍石U-Pb (153±2)	Pan et al., 2017；于全等, 2018
小柳沟	矽卡岩W-Mo(Cu)	甘肃	$w(WO_3)$ 487 600 t, 0.4%	二长花岗岩、花岗闪长岩	Re-Os (427.4±6.0)、(428.2±6.0)；Ar-Ar (392.0±2.7)、(391.1±2.7)、(391.4±2.8)	Zheng et al., 2017
白干湖	矽卡岩W-Sn	新疆	$w(WO_3)$ 174 913 t; w(Sn) 79 091 t	正长花岗岩	Ar-Ar (411.7±2.6)、(412.8±2.4)、(413.8±2.6)	Zhou et al., 2016a
锡田	矽卡岩W-Sn	湖南	$w(WO_3)$ 46 300 t, 0.28%~0.63%; w(Sn) 586 000 t, 0.26%~0.36%	黑云母花岗岩	Re-Os (150±2.7)；Ar-Ar (155.6±1.3)、(157.2±1.4)	Zhou et al., 2015；Zhao et al., 2017
柿竹园	矽卡岩-云英岩型W-Sn(F, Mo)	湖南	$w(WO_3)$ 800 000 t, 0.35%; w(Sn) 486 000 t, 0.36%; w(Mo) 200 000 t, 0.07%; w(Bi) 100 000 t, 0.17%	黑云母(电气石)花岗岩	Ar-Ar (153.7±0.9)；Re-Os (151.0±3.5)；Sm-Nd (149±2)	Lu et al., 2003；Zhao et al., 2017
瑶岗仙	矽卡岩-石英脉型W-Mo	湖南	$w(WO_3)$ 236 000 t, 1.27%	二云母花岗岩	Re-Os(154.9±2.6)；Ar-Ar(153.0±1.1)、(155.1±1.1)	Peng et al., 2006
新田岭	矽卡岩-石英脉型W-Mo-Pb-Zn	湖南	$w(WO_3)$ 300 000 t, 0.37%	黑云母花岗岩、黑云母二长岩	Rb-Sr (157.4±3.2)；Re-Os (161.7±9.3)	蔡明海等, 2008；袁顺达等, 2012
黄沙坪	矽卡岩W-Mo-Cu-Pb-Zn	湖南	$w(WO_3)$ 152 900 t, 0.2%; w(Mo) 43 200 t, 0.2%; w(Pb) 761 300 t, 3.55%; w(Zn) 15 291 t, 7.13%	花岗斑岩	Re-Os (154.8±1.9)、(153.8±4.8)、(159.4±3.3)、(157.5±2.4)	Zhao et al., 2017
魏家	矽卡岩W	湖南	$w(WO_3)$ 300 000 t, 0.12%	花岗斑岩、石英斑岩	Re-Os (159.0±5.6)	Zhao et al., 2016
努日	矽卡岩W-Cu	西藏	WO_3 0.280%; Cu 0.694%	石英闪长玢岩、黑云母花岗岩	Re-Os (24.27±0.55)	陈雷, 2011
夜长坪	矽卡岩-斑岩型Mo-W	河南	w(Mo) 250 000 t, 0.133%	钾长花岗斑岩	Re-Os (145.3±4.4)	毛冰等, 2010
三道庄	矽卡岩W-Mo	河南	$w(WO_3)$ 555 000 t, 0.112%; w(Mo) 750 000 t, 0.109%	花岗斑岩	Re-Os (145.0±2.2)	李永峰等, 2003
上房	矽卡岩-石英脉型W	福建	$w(WO_3)$ 50 000 t, 0.2%	黑云母正长花岗岩	Re-Os (158.1±5.4)	Zhao et al., 2017
弓棚子	矽卡岩W-Cu-Zn	黑龙江	–	黑云母花岗岩、花岗闪长岩	Re-Os(176.7±0.9)	Li et al., 2019
翠宏山	矽卡岩-斑岩型W-Mo-Pb-Zn(Fe-Cu)	黑龙江	$w(WO_3)$ 120 000 t; w(Fe) 39 400 000 t; w(Mo) 90 000 t; w(Pb) 190 000 t; w(Zn) 510 000 t; w(Cu) 30 000 t	石英二长岩、黑云母二长花岗岩、斑状花岗岩	锡石U-Pb(195.4±1.9)、(191.2±7.5)	Fei et al., 2018
焦里	矽卡岩W-Ag-Pb-Zn	江西	$w(WO_3)$大于50 000 t, 0.34%; w(Pb+Zn)大于300 000 t, Pb 1.17%；Zn 0.75%	花岗闪长岩	Re-Os (170.6±4.6)	丰成友等, 2012
香炉山	矽卡岩W(Au, Ag, Cu, Pb)-Zn	江西	$w(WO_3)$ 220 000 t, 0.641%	黑云母花岗岩	Sm-Nd (121±11)；Re-Os (125.5±0.7)；Ar-Ar (122.8±0.78)	Dai et al., 2018

续表 1

Continued Table 1

矿床	矿床类型和矿化元素	国家或地区	储量及品位	成矿岩体	成矿时代/Ma	资料来源
百丈岩	矽卡岩-斑岩型 W-Mo	安徽	$w(WO_3)$ 20 000 t; w(Mo) 10 000 t	二长岩、细粒花岗岩	Re-Os (136.3±2.6)	秦燕等, 2010
高家塝	矽卡岩-斑岩型 W-Mo(Au)	安徽	$w(WO_3)$ 62 000 t; w(Mo) 5400 t	花岗闪长岩、花岗斑岩、二长斑岩	Re-Os (146.1±4.8)	肖鑫等, 2017; Song et al., 2019
牛塘界	矽卡岩W	广西	0.4%	白云母花岗岩	Sm-Nd (421±24) 锡石 U-Pb (420.8±8.0)	Chen et al., 2018
社洞	矽卡岩-斑岩-石英脉型 W-Mo	广西	WO_3 0.06%~4.63%;Mo 0.03%~0.43%	花岗闪长(斑)岩	Re-Os (437.8±3.4)	陈懋弘等,2011
Cantung	矽卡岩W-Cu(Zn)	加拿大	$w(WO_3)$ 4 200 000 t, 1.6%	黑云母二长花岗岩、白岗岩	锆石 U-Pb (96.7±0.6)、(98.2±0.4)、(101.15±0.44)	Rasmussen et al., 2011
Mactung	矽卡岩-云英岩型 W-Cu(Zn)	加拿大	$w(WO_3)$ 33 000 000 t, 0.88%	黑云母石英二长岩	Re-Os (97.5±0.5)	Selby, 2003; Brown et al., 2014
King Island	矽卡岩W	澳大利亚	$w(WO_3)$ 6 580 000 t, 0.64%~0.8%	花岗(闪长)岩	榍石裂变径迹 (350)	Gleadow et al., 1978
Pine Creek	矽卡岩W	美国	$w(WO_3)$大于6 000 000 t	石英二长岩	94、200	Brown et al., 1985
Sangdong	矽卡岩W-Mo	朝鲜	$w(WO_3)$ 9 520 000 t, 0.56%	花岗岩	Ar-Ar (86.6±0.2)、(87.5±4.5)	Seo et al., 2017
Los Santos	矽卡岩W	西班牙	$w(WO_3)$ 3 090 000 t, 0.54%	黑云母二长花岗岩、黑云母花岗闪长岩	K-Ar (281±6~280±6)、(270±6~269±6)	Sánchez et al., 2009
Vostok-2	矽卡岩W-Cu	俄罗斯	$w(WO_3)$大于180 000 t, 1.7%	花岗闪长岩、二长花岗岩、花岗斑岩	Rb-Sr (104±6)、(101±1)	Soloviev et al., 2017

性均有出现,而斑岩型以及花岗岩型钨矿的成矿岩体相对更加富碱(图3a)。A/CNK集中在0.9~1.8,属于准铝质、强过铝质花岗岩,其中与矽卡岩型钨矿有关的花岗岩铝饱和指数相对更高(图3b)。Ballouard等(2016)总结指出,Nb/Ta和Zr/Hf比值可以作为岩浆-热液反应或者分离结晶,以及花岗质岩石成矿潜力的标志。大部分与钨矿床有关的花岗质岩石的Zr/Hf比值落在了Zr/Hf<46的含矿花岗岩区域(图3c)。其中,与石英脉型钨矿床有关的花岗质岩石具有明显较低的Nb/Ta(大部分<4)和Zr/Hf(大部分<26)比值;与斑岩型、花岗岩型以及变质成因的钨矿床有关的岩体则具有相对较高的Nb/Ta(1~10)和Zr/Hf(10~40)比值;而与矽卡岩型钨矿床有关的花岗质岩体的Nb/Ta(1~11)和Zr/Hf(6~46)比值变化较为宽泛,暗示大部分钨矿床的成矿岩体与岩浆-热液作用关系密切(Bau, 1996; Ballouard et al., 2016;吴福元等,2017)。钨成矿岩体的稀土元素配分模式可以划分为"斜倾式"和"海鸥式"2种类型,且同一矿床的成矿岩体可能同时具有上述2种类型。"斜倾式"花岗岩明显富集轻稀土元素,具有较弱-中等的负Eu异常;"海鸥式"花岗岩轻、重稀土元素分异不明显,具有强烈的负Eu异常,同时部分"海鸥式"花岗岩的稀土元素还呈现明显的四组分效应,表明发生了熔体-流体反应(李献华等, 2007; Guo et al., 2012; Jiang et al., 2016)。

华南与W-Sn矿有关的燕山期花岗岩呈现S型、I型或A型花岗岩的特征(Chen et al., 2013),可能源于地壳±岩石圈地幔的部分熔融,并受到地壳沉积物质的混染(Zhou et al., 2006; Zhang et al., 2017),或者分异于中下地壳镁铁质火成源岩并且可能有少量新生地壳和/或地幔分异物质加入(Zhou et al., 2006; 李献华等,2007),且多受古太平洋大洋岩石圈俯冲作用的影响。而与W-Sn矿化有关的加里东期花岗岩则多呈现S型花岗岩的特征(Chen et al., 2018),源于古元古代大陆地壳的重熔(Li et al., 2017),形成于陆内造山的挤压或者伸展环境(李晓峰等,2012)。Chen等(2013)指出南岭加里东期钨矿基本以白钨矿为主,认为可能受到了加里东期花岗岩的物源及成岩条件的控制。研究表明,控制W、Sn、Nb、Ta、Li、Be等金属元素在花岗岩类中富集的因素主要包

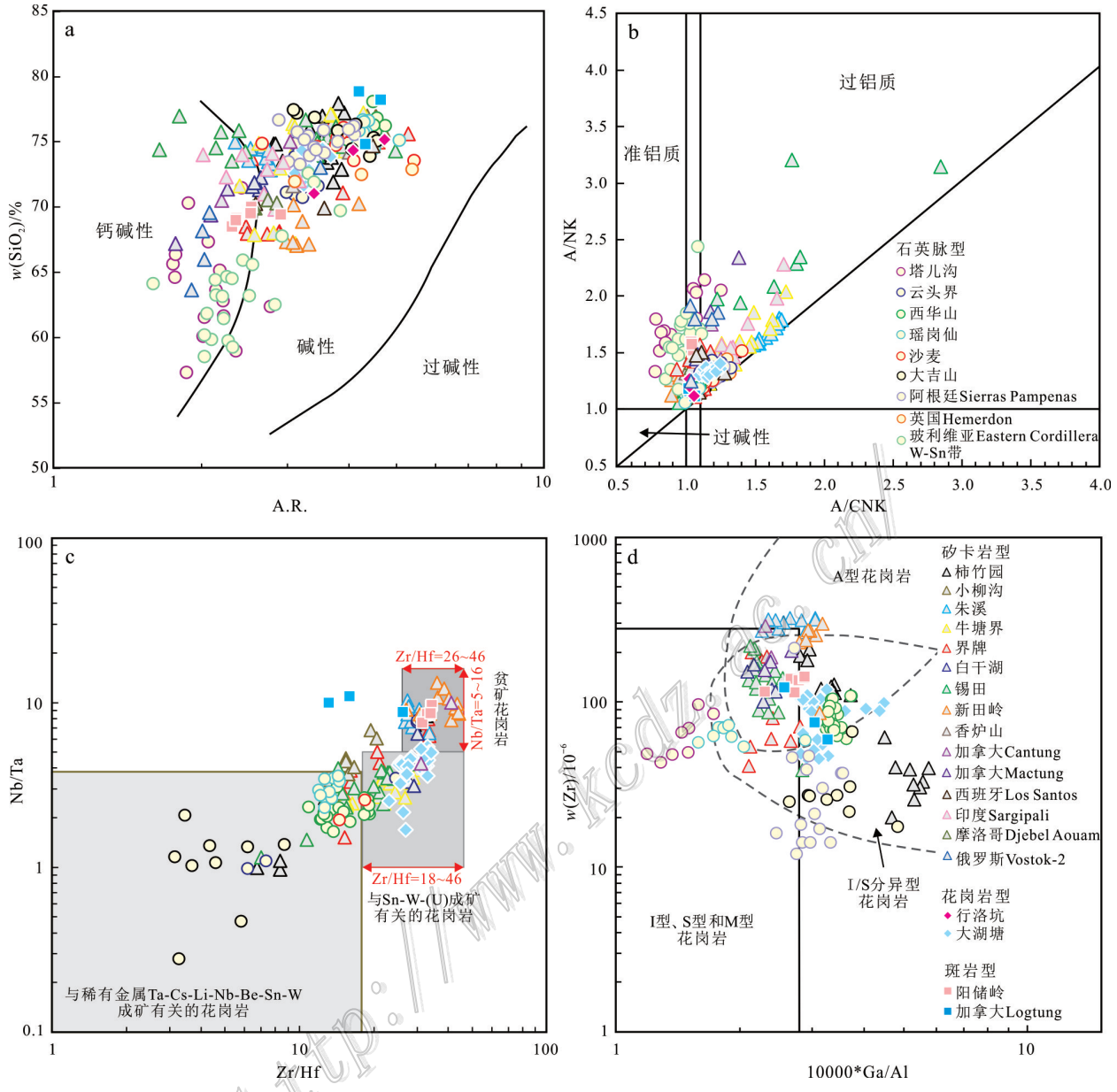

图3 与钨矿床有关的岩石地球化学图解(c据Ballouard et al., 2016;d据Whalen et al., 1987; 吴福元等, 2017修改)

a. SiO_2 vs. A.R.($w(Al_2O_3+CaO+Na_2O+K_2O)/w(Al_2O_3+CaO-Na_2O-K_2O)$); b. A/NK vs. A/CNK; c. Nb/Ta vs. Zr/Hf; d. Zr vs. 10000×Ga/Al,数据引自Sugaki et al., 1988; Giuliani et al., 1987; Mao et al., 2017; Brand, 2008; Chowdhury et al., 2011; Rasmussen et al., 2011; Fogliata et al., 2012; Guo et al., 2012; 董少花等, 2014; Mao et al., 2015; Chen et al., 2016; Jiang et al., 2016; 林书平, 2016; Zhou et al., 2015; Zhou et al., 2016a; Huang et al., 2017; Simons et al., 2017; Soloviev et al., 2017; Zheng et al., 2017; Chen et al., 2018

Fig. 3 Geochemical diagrams of the host rocks associated with tungsten deposits (c modified after Ballouard et al., 2016; d modified after Whalen et al., 1987; Wu et al., 2017)

a. SiO_2 versus A.R.; b. A/NK versus A/CNK; c. Nb/Ta versus Zr/Hf; d. Zr versus 10000×Ga/Al

Data after Sugaki et al., 1988; Giulianli et al., 1987; Mao et al., 2017; Brand, 2008; Chowdhury et al., 2011; Rasmussen et al., 2011; Fogliata et al., 2012; Guo et al., 2012; Dong et al., 2014; Mao et al., 2015; Chen et al., 2016; Jiang et al., 2016; Lin, 2016; Zhou et al., 2015; Zhou et al., 2016a; Huang et al., 2017; Simons et al., 2017; Soloviev et al., 2017; Zheng et al., 2017; Chen et al., 2018

括,物源组成(Romer et al., 2014)、结晶分异程度(Taylor et al., 1992)以及后期的热液叠加作用(Haapala, 1997)。然而,由于针对W等元素在源岩融化和过铝质花岗岩岩浆演化过程中的研究较为有限,因此,具体是哪些成岩过程,例如结晶分异作用、岩浆混合作用、地壳混染和/或与花岗质熔体相关的热

液活动,控制了含钨花岗岩和相关钨矿化的形成还未研究清楚(Zhang et al., 2017)。

4　矽卡岩型钨矿的成矿作用

4.1　成矿流体特征

矽卡岩矿床的成矿作用存在多期次多阶段演化的特征(Meinert et al., 2003),其成矿流体的温度(T)和盐度($w(NaCl_{eq})$)变化范围较大。早期矽卡岩阶段的成矿流体显示高温(400~700℃)和高盐度($w(NaCl_{eq})$>50%)的岩浆来源特征。值得注意的是,一些矽卡岩型钨矿的早期矽卡岩矿物中的流体包裹体存在相对较低的均一温度,如中国华南宝山矽卡岩型白钨矿矿床中无水矽卡岩阶段晚期的矿物包裹体均一温度范围为 197~377°C(Zhao et al., 2018)。这些暗示着早期矽卡岩阶段的流体并不一定完全继承了岩浆流体的高温特征。晚期退化蚀变阶段的成矿流体具有更低的温度(200~400℃)和低盐度($w(NaCl_{eq})$≤20%),但仍以岩浆来源为主(Singoyi et al., 2000; Meinert et al., 2005)。白钨矿在早期矽卡岩阶段和晚期退化蚀变阶段均可发育,但其形成伴随退蚀变作用达到顶峰,沉淀温度多介于250~400℃。矽卡岩型钨矿的成矿流体存在中-高盐度和中-低盐度 2 种类型:氧化的矽卡岩(-斑岩)型钨矿的矽卡岩期普遍发育高盐度包裹体,并且该类型包裹体可能同时与富气相中-低盐度包裹体共存而形成沸腾包裹体组合(Lu et al., 2003; Li et al., 2016; Orhan, 2017);而还原的矽卡岩型钨矿则具有上述 2 种不同的盐度特征(Mathieson et al., 1984; Soloviev et al., 2017)。相对比而言,石英脉型和花岗岩型白钨矿矿床的成矿流体一般为中-低盐度流体,并具有一定量的 CO_2±CH_4(Graupner et al., 1999; Seo et al., 2017; Wang et al., 2017; Xie et al., 2018),暗示成矿环境偏酸性且可能缺少明显的沸腾作用使 CO_2 逃逸。

4.2　钨的分配、迁移与沉淀

在自然体系中,钨具有较高的流体亲和性(流体/熔体分配系数 1~5,Zajacz et al., 2008;Hulsbosch et al., 2016)和中等不相容的熔体亲和性(晶体/熔体分配系数约 0.4,Hulsbosch et al., 2016),这会导致在熔体分异过程中钨倾向于富集在共存的流体相,从而在岩浆流体饱和的初始阶段,流体中的钨就有很大的成矿潜力(Hulsbosch, 2019)。针对不同条件下溶液-熔体中钨的分配行为的实验研究表明,约束其流体/熔体分配系数(D_w)的主要因素有温度、压力(P)、熔体组分、氧逸度($f(O_2)$)和挥发分(H_2O、Cl^-、F^-、CO_3^{2-})等(Bai et al., 1999;Wood et al., 2000; Zajacz et al., 2008)。流体包裹体成分分析可以提供关于岩浆卤水-气相分离过程对金属元素的选择性迁移作用和导致矿石矿物沉淀的化学反应以及物理过程等方面的信息(Audétat et al., 1998)。Heinrich 等(1999)利用 LA-ICP-MS 技术分析岩浆-热液矿床中流体包裹体的主微量元素发现,Na、K、Fe、Mn、Zn、Rb、Cs、Pb (Ag、Tl、Bi、Ba、Sr、Sn、W、U、Ce)倾向于进入卤水溶液相,可能以 Cl 络合物形式存在;Cu、As、Au、B(Sb、S、Li)则选择性进入气相,其中,金属元素可能以 HS 络合物形式存在。

钨等金属元素在热液流体中的迁移可能受到源岩、围岩成分和流体物化条件(如 T、P、pH 值)等因素影响。大量实验研究指出,钨的迁移形式有氯化物、氟化物和碳酸盐络合物,以及同多钨酸盐和杂多钨酸盐等(Foster, 1977; Higgins, 1980; Manning et al., 1984; Keppler et al., 1991; Gibert et al., 1992; Wood et al., 2000; Lowenstern, 2001)。在高温热水溶液中,氯化物、氟化物和碳酸盐络合物形式对钨的迁移起到了重要作用,但它们不是必需的。同多钨酸盐和杂多钨酸盐形式,如 $H_6[H_2W_{12}O_{40}]$、$H_3[PW_{12}O_{40}]$、$HW_6O_{21}^{5-}$、$H_2WO_4^0$、HWO_4^-、WO_4^{2-}、$NaHWO_4^0$ 和 $NaWO_4^-$ 等,同样可以迁移足量的钨而形成钨矿床(Foster, 1977; Manning et al., 1984; Wood et al., 2000)。值得注意的是,F 的存在可以降低花岗质岩浆的黏度和固相线温度,起到岩浆解聚和延长岩浆结晶过程的作用,从而提高了岩浆演化的程度和熔体中钨的富集程度,延缓了含钨热液从岩浆中的分离,但 F 的存在本身可能与钨的溶解和迁移无关(Audétat et al., 2000; Linnen et al., 2005; Che et al., 2013a)。

控制钨矿物沉淀的因素本质上包括:① 成矿流体的组成变化,如溶液中离子活度比值($\alpha(Ca^{2+})/(\alpha(Fe^{2+})+\alpha(Mn^{2+}))$、NaCl 含量和 X_{CO_2} 等;② 成矿环境的物理化学条件变化,如 T、P、pH 值和 $f(O_2)/f(S_2)$ 等(Foster, 1977; Wood et al., 2000)。目前研究提出了很多钨矿物的沉淀机制,主要包括:① 降温(Ni et al., 2015),但需要注意的是,在 100~500℃范围内,白钨矿的溶解度随着温度降低而增加,暗示单独的降温过程可能不是白钨矿矿床形成的有效因素(Foster, 1977; Wood et al., 2000);② 流体-围岩反

应，主要伴随着pH值增加、T降低和Ca的富集（Mathieson et al., 1984; Wang et al., 2017）以及围岩中非极性挥发分的加入（Gibert et al., 1992; O'Reilly et al., 1997）；③ 流体混合，及其可能伴随的$f(O_2)$和pH值增加，T和流体Cl含量降低（Linnen et al., 1994; Singoyi et al., 2001;Wei et al., 2012）；④ 流体不混溶以及流体沸腾和/或CO_2泡腾，及其导致的P降低和pH值升高（Lu et al., 2003; Korges et al., 2017; Orhan, 2017; Soloviev et al., 2017）。其中，流体-围岩反应被认为是形成钨矿床的关键机制（Lecumberri-Sanchez et al., 2017），流体沸腾和流体混合作用被认为是形成具有异常高品位钨矿床的主要机制（Wei et al., 2012; Korges et al., 2017），且同一矿床中钨矿物的沉淀通常受多种机制协同作用。

4.3 成矿物质来源

目前，研究主要利用同位素分析直接约束矽卡岩型钨矿的成矿物质来源，包括C-H-O-S稳定同位素（Bowman et al., 1985; Zaw et al., 2000; Li et al., 2016），Sr-Nd-Pb放射性同位素（Song et al., 2014; Li et al., 2016）以及流体包裹体He-Ar同位素。

对于矽卡岩型钨矿的成矿物质来源仍存在一定争议，大部分学者认为矽卡岩矿床的成矿物质属于岩浆来源（Bowman et al., 1985; Brown et al., 1985），而另一些学者认为是地层和岩浆混合来源（Ishihara et al., 2003），同时，还有少数学者认为成矿物质仅仅来源于围岩地层，如层控矽卡岩型钨矿（Skaarup, 1974）。Meinert等（2005）总结矽卡岩型钨矿的稳定同位素研究指出，根据早期矽卡岩矿物组合的C-O同位素及其形成温度所估算的热液流体具有沉积成因$\delta^{18}O$、$\delta^{13}C$值和岩浆$\delta^{18}O$、$\delta^{13}C$值混合的特征，表明大部分该类型矿床形成于多元流体。何兴华等（2017）总结了华南中生代典型石英脉型、矽卡岩型、斑岩型以及云英岩型钨矿床中成矿流体的He-Ar和H-O同位素特征，结果显示不同类型的钨矿床的成矿流体具有不同程度的壳源-幔源混合特征，除了主要的岩浆水外还普遍存在不同程度的大气降水的加入。其中，矽卡岩型钨矿的成矿流体具有最为明显的大气降水的参与并且可能存在一定地幔组成的加入。相对比而言，石英脉型、斑岩型以及蚀变花岗岩型白钨矿的成矿流体则多呈现壳源特征以及岩浆水和少量大气降水混合的特点（Xie et al., 2018）。

5 矽卡岩型钨矿矿物学

矽卡岩矿物组合是研究矽卡岩矿床分带的重要依据，其结构构造和化学成分对于理解矽卡岩矿床的成因、示踪流体性质和矿化过程中环境变化具有重要的指示意义。早期研究主要将石榴子石和辉石成分作为不同矿种的指标，如赵斌等（1987）研究认为石榴子石和辉石成分与矽卡岩型矿床的金属矿化类型有关，中国矽卡岩型矿床中的石榴子石主要为（铁铝榴石+镁铝榴石+锰铝榴石）（Al+Sp+Py）总含量低于15%的铬钙铁榴石系列。只有Sn-W钙矽卡岩型矿床及Pb-Zn钙镁矽卡岩型矿床发育（Al+Sp+Py）总含量大于15%的贫钙石榴子石。由于矽卡岩型钨矿的围岩、侵入体氧逸度和形成深度均与其他矽卡岩型矿床不同，使其主要呈现中等-低的氧化还原状态，因此，钨矽卡岩多发育贫钙质石榴子石（Newberry, 1983）。Meinert等（2005）统计不同矿化类型矽卡岩中的石榴子石和辉石主成分特征也指出，钨矽卡岩常见贫钙石榴子石和富铁辉石。近年来，单个矿物颗粒形成过程中主微量元素和同位素成分的变化所反映的流体组分、物理化学条件和矿物生长动力学等方面的信息以及U-Pb定年是矽卡岩石榴子石研究的热点（Smith et al., 2004; Gaspar et al., 2008;Deng et al., 2017;Park et al., 2017; Seman et al., 2017）。矽卡岩中的热液石榴子石多发育生长环带，是体系对流体保持开放的典型结果，它记录了热液流体体系地球化学演化的全部过程。石榴子石的O同位素可以示踪其形成过程中的流体来源，结合Fe-Al成分环带特征可以解释宏观的矽卡岩形成过程中流体成分、氧化还原状态以及流体来源的特征与演化（Crowe et al., 2001）。W、Sn、Mo等金属元素在矽卡岩石榴子石中较为罕见，但是高W含量（w(W)高达2700×10^{-6}）的石榴子石已经在矽卡岩型矿床中有所报告，如西藏知不拉矽卡岩型铜矿（Xu et al., 2016）。然而，有关矽卡岩型钨矿中石榴子石的研究显示，它们普遍不具有显著的w(W)（$<5\times10^{-6}$, Zhou et al., 2016a; Ding et al., 2018），除了韩国Weondong矽卡岩型钨矿中石榴子石w(W)高达458×10^{-6}（Park et al., 2017）。因此，石榴子石的W含量可能不可用于指导矽卡岩钨矿勘探。辉石作为另一个主要的矽卡岩矿物，普遍富集Co、Zn、Ti、Cr、Ni、V等不相容元素，针对不同类型的辉石的微量元素研究

可以明确矽卡岩矿物组合间元素的富集和配分规律,以及约束流体的演化过程(Ismail et al., 2014)。角闪石和帘石类矿物作为矽卡岩矿床中典型的含水矿物,其研究也具有一定的指示意义。如 Meinert 等(2005)总结指出,Cu、Au、W 以及 Sn 矽卡岩中的角闪石相对富 Al,Cu、Mo 和 Fe 矽卡岩中的相对富集 Fe,而 Zn 矽卡岩中的相对富集 Mn 和亏损 Ca。而帘石类矿物中不同矿物类型则在一定程度上反映了氧化还原条件的差异,如绿帘石(Fe^{3+})和黝帘石(Fe^{2+})分别暗示了相对氧化和还原的环境。此外,矽卡岩型钨矿中的榍石普遍富集 W、Sn 和 Nb,可以用于指示钨矿勘探(Che et al., 2013b)。

白钨矿作为矽卡岩型钨矿中主要的矿石矿物,能够提供成矿的直接信息。不同地球化学类型的白钨矿(如矽卡岩型、石英脉型以及斑岩型或云英岩型)可以同时出现在同一个岩浆热液体系中,因此,其地球化学成分(稀土元素以及其他微量元素,尤其是 Mo 和 Sr)的连续性变化可以提供整个矿床尺度上流体演化的全面信息(如物化条件以及物质组成的改变),有助于更好地揭示矿床的成因。白钨矿多呈现不同的阴极发光强度,主要与白钨矿的 Mo 含量呈负相关关系,并且白钨矿阴极发光的岩相学特征与矿床形成背景具有直接联系(Poulin et al., 2018):变质成因的矿床中(如造山型金矿)的白钨矿的阴极发光较为均一,而岩浆成因的矿床中(如矽卡岩型钨矿)的白钨矿的阴极发光则具有明显的环带特征。近年来,在详细的 SEM-BSE 或 CL 岩相学研究基础上,主要针对白钨矿的微量元素和同位素特征开展了一定研究:① 采用 LA-ICP-MS 或 SIMS 的联用技术对白钨矿的原位微量元素(Ghaderi et al., 1999; Brugger et al., 2000; Zhao et al., 2017; Poulin et al., 2018; Sun et al., 2019)和 Sr 或 O 同位素进行分析(Shelton et al., 1987; Brugger et al., 2002; Kozlik et al., 2016; Scanlan et al., 2018; Song et al., 2019),用以判断形成化学成分不均一的白钨矿颗粒的流体特征、来源及其演化。Poulin 等(2018)提出白钨矿的 Sr、Mo 和 Eu_A(Eu_A versu Sr/Mo 投图)可以用来初步鉴别白钨矿的矿床成因类型,并且白钨矿的晶体化学可以很好地指示其成矿环境。② 采用 ID+TIMS 测试手段分析白钨矿的 Sr-Nd-Pb 同位素特征以及 Sm-

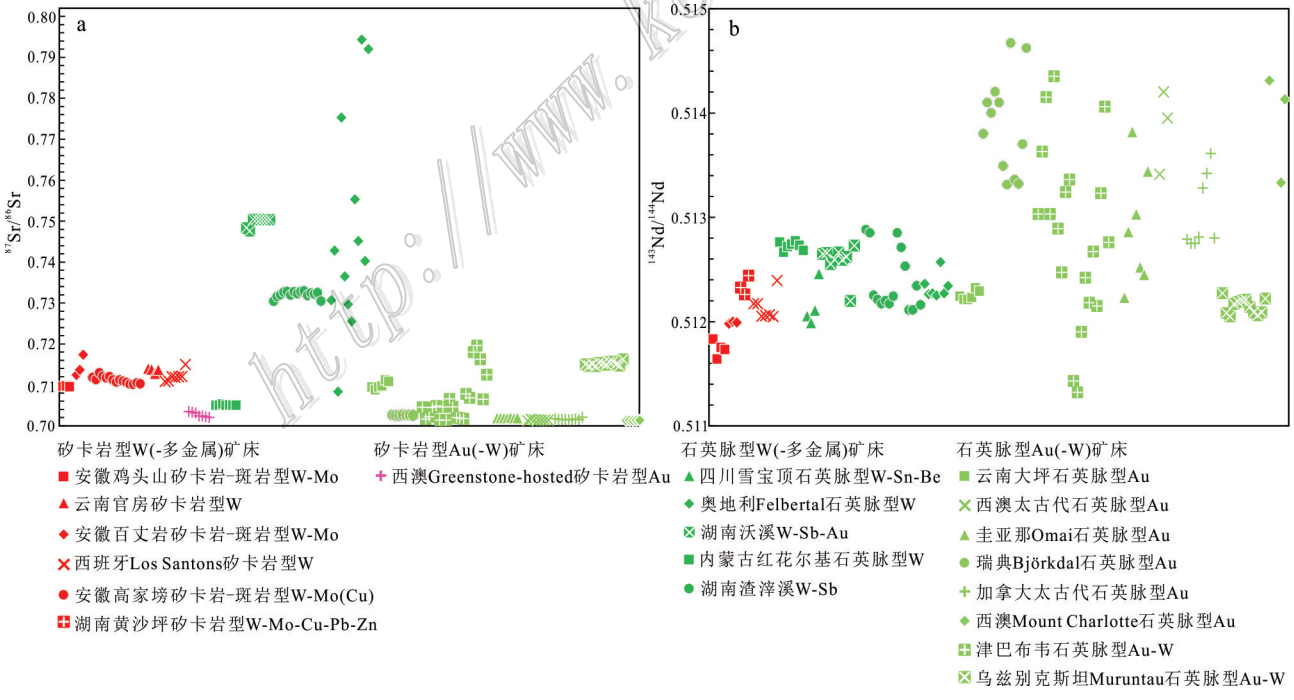

图 4　不同成因类型矿床中白钨矿的 $^{87}Sr/^{86}Sr$(a)和 $^{143}Nd/^{144}Nd$(b)同位素组成(数据引自 Mueller et al., 1991; Roberts et al., 2006; Liu et al., 2007; Tornos et al., 2008; Song et al., 2014, 2019; Guo et al., 2016; Kozlik et al., 2016; Li et al., 2016; Zhang et al., 2016)

Fig. 4　Plot of $^{87}Sr/^{86}Sr$ (a) and $^{143}Nd/^{144}Nd$ (b) in scheelite from deposits of different genetic types(data after Mueller et al., 1991; Roberts et al., 2006; Liu et al., 2007; Tornos et al., 2008; Song et al., 2014, 2019; Guo et al., 2016; Kozlik et al., 2016; Li et al., 2016; Zhang et al., 2016)

Nd年龄。白钨矿的初始Sr同位素可以估测成矿流体的Sr同位素组成(Kempe et al., 2001)和反应成矿流体的流动轨迹(Voicu et al., 2000);Nd同位素可以示踪成矿流体来源(Tornos et al.,2008; Song et al., 2014;Sun et al., 2017)以及复杂的多变质背景下的W矿化作用的演化(Eichhorn et al.,1997)。白钨矿普遍具有分散变化的Sm/Nd比值,可能源于形成白钨矿的流体成分具有不断变化的特征(Brugger et al., 2002; Peng et al., 2004)。此外,Song等(2014)通过系统对比研究指出,白钨矿的Sr-Nd同位素组成可以判别矿床的成因类型,即矽卡岩型W(-多金属)矿床中的白钨矿具有相对中等的$^{87}Sr/^{86}Sr$比值和最低的$^{143}Nd/^{144}Nd$比值,石英脉型W(-多金属)矿床中的白钨矿具有最高的$^{87}Sr/^{86}Sr$比值和中等的$^{143}Nd/^{144}Nd$比值,而石英脉型Au(-W)矿床中的白钨矿具有最低的$^{87}Sr/^{86}Sr$比值和最高的$^{143}Nd/^{144}Nd$比值,且矽卡岩型Au矿中的白钨矿也相对矽卡岩型W矿中的白钨矿呈现更低$^{87}Sr/^{86}Sr$比值(图4a、b),主要受不同的成矿物质来源控制(地幔物质、地壳物质、赋矿围岩以及深源岩浆)。而不同成因类型的矿床中的白钨矿O同位素值互相重叠,范围为−4.6~12.7‰,因此,白钨矿的O同位素组成本身不能指示特定矿床类型的成矿流体O同位素特征(Poulin et al., 2018)。白钨矿($CaWO_4$)和钼钙矿($CaMoO_4$)之间存在一个非理想固溶体系列,Xu等(2019)利用HAADF-STEM(high-angular annular dark field scanning-TEM)研究了西藏知不拉矿床类矽卡岩中的白钨矿-钼钙矿固溶体,发现具有不同化学组成的振荡环带具有连续的晶体定向。并且在该固溶体中还发现nm级的针状磷钇矿,有助于更好地利用白钨矿的稀土元素含量以及配分模式解释相关成岩成矿问题。

6 结 论

(1)针对矽卡岩矿物以及白钨矿和黑钨矿等钨矿物的直接定年分析对于约束矽卡岩矿床的岩浆-热液活动持续时间和演化历史至关重要。目前,LA-ICP-MS石榴子石U-Pb定年技术开发的标样主要为钙铁榴石,但矽卡岩型钨矿中普遍发育钙铝榴石以及贫钙石榴石子石,因此,仍需要开发钙铝榴石甚至贫钙石榴石子石标样。此外,利用LA-ICP-MS黑钨矿U-Pb定年技术直接约束W-Sn矿的形成年龄已取得成功。而对于白钨矿来说,主要以Sm-Nd定年为主,该方法误差普遍较大并且获得的结果可能是混合年龄。Wintzer等(2016)提出了利用LA-ICP-MS原位技术分析白钨矿U-Pb年龄的可能性,表明未来应该着重建立LA-ICP-MS白钨矿U-Pb定年方法。

(2)在钨矿床中,往往是多个因素共同影响钨矿物的沉淀,查明不同阶段的主要沉淀机制有助于更好地理解钨的富集成矿规律。应在详细的野外和室内岩相学研究基础上,联合SEM-CL对白钨矿环带中的流体包裹体进行准确的测温、激光拉曼以及LA-ICP-MS微量元素分析,查明与钨矿化有关的成矿流体期次,成矿环境和成矿流体成分的特点及变化,更有针对性地探讨钨的成矿环境和成因机制。

(3)矽卡岩型矿床的成矿作用普遍存在多期次多阶段演化的特征。应当针对不同阶段的钨矿化,运用微区O-Sr-Pb同位素以及非传统同位素(如Mo、Cu、Sn、W等)等手段,厘清不同期次不同阶段的成矿流体及物质来源,更加深入和细致地认识钨的源区特征。

References

Audétat A, Gunther D and Heinrich C A. 1998. Formation of a magmatic-hydrothermal ore deposit: Insights with LA-ICP-MS analysis of fluid inclusions[J]. Science, 279(5359): 2091-2094.

Audétat A, Günther D and Heinrich C A. 2000. Magmatic-hydrothermal evolution in a fractionating granite: A microchemical study of the Sn-W-F-mineralized Mole granite (Australia)[J]. Geochimica et Cosmochimica Acta, 64: 3373-3393.

Bai T B and Van Groos A F K. 1999. The distribution of Na, K, Rb, Sr, Al, Ge, Cu, W, Mo, La, and Ce between granitic melts and coexisting aqueous fluids[J]. Geochimica et Cosmochimica Acta, 63(7): 1117-1131.

Ballouard C, Poujol M, Boulvais P, Branquet Y, Tartèse R and Vigneresse J L. 2016. Nb-Ta fractionation in peraluminous granites: A marker of the magmatic-hydrothermal transition[J]. Geology, 44: 231-234.

Bau M. 1996. Controls on the fractionation of isovalent trace elements in magmatic and aqueous systems: Evidence from Y/Ho, Zr/Hf, and lanthanide tetrad effect[J]. Contributions to Mineralogy and Petrology, 123: 323-333.

Bi C S. 1987. Basic geological characteristics of skarn-type scheelite deposit in China[J]. Bulletin of the Chinese Academy of Geological Sciences, 17(3): 49-64(in Chinese with English abstract).

Bowman J R, Covert J J, Clark A H and Mathieson G A. 1985. The

Cantung E Zone scheelite skarn orebody, Tungsten, northwest Territories; oxygen, hydrogen, and carbon isotope studies[J]. Econ. Geol., 80(7): 1872-1895.

Brand A A. 2008. Mineralogy, geochemistry, and geochronology of the northern Dancer tungsten-molybdenum deposit, Yukon and British Columbia (doctoral dissertation)[D]. Supervisor: Lee G. Vancouver: University of British Columbia.46-52.

Breiter K, Škoda R and Uher P. 2007. Nb-Ta-Ti-W-Sn-oxide minerals as indicators of a peraluminous P-and F-rich granitic system evolution: Podlesí, Czech Republic[J]. Mineralogy and Petrology, 91 (3-4): 225-248.

Breiter K. 2012. Nearly contemporaneous evolution of the A- and S-type fractionated granites in the Krušnéhory/Erzgebirge Mts. Central Europe[J]. Lithos, 151: 105-121.

Brown P E, Bowman J R and Kelly W C. 1985. Petrologic and stable isotope constraints on the source and evolution of skarn-forming fluids at Pine Creek, California[J]. Econ. Geol., 80(1): 72-95.

Brown T and Pitfield P. 2014. Critical metals handbook[A]. In: Gunn G, ed. Tungsten[C].New York: John Wiley and Sons. 397-425.

Brugger J, Lahaye Y, Costa S, Lambert D and Bateman R. 2000. Inhomogeneous distribution of REE in scheelite and dynamics of Archaean hydrothermal systems (Mt. Charlotte and Drysdale gold deposits, western Australia)[J]. Contributions to Mineralogy and Petrology, 139(3): 251-264.

Brugger J, Maas R, Lahaye Y, McRae C, Ghaderi M, Costa S, Lambert D, Bateman R and Prince K. 2002. Origins of Nd-Sr-Pb isotopic variations in single scheelite grains from Archaean gold deposits, western Australia[J]. Chemical Geology, 182(2-4): 203-225.

Cai M H, Han F B, He L Q, Liu G Q, Chen K X and Fu J M. 2008. He, Ar isotope characteristics and Rb-Sr dating of the Xintianling Skarn scheelite deposit in southern Hunan, China[J]. Acta Geoscientica Sinica, 29(2): 167-173(in Chinese with English abstract).

Che X D, Linnen R L, Wang R C, Aseri A and Thibault Y. 2013a. Tungsten solubility in evolved granitic melt: An evaluation of magmatic wolframite[J]. Geochimica et Cosmochimca Acta, 106: 84-98.

Che X D, Linnen R L, Wang R C, Groat L A and Brand A A. 2013b. Distribution of trace and rare earth elements in titanite from tungsten and molybdenum deposits in Yukon and British Columbia, Canada[J]. The Canadian Mineralogist, 51(3): 415-438.

Chen G H, Shu L S, Shu L M, Zhang C and Ouyang Y P. 2016. Geological characteristics and mineralization setting of the Zhuxi tungsten (copper) polymetallic deposit in the eastern Jiangnan Orogen[J]. Science China, 59(4): 803-823.

Chen J, Wang R C, Zhu J C, Lu J J and Ma D S. 2013. Multiple-aged granitoids and related tungsten-tin mineralization in the Nanling Range, South China[J]. Science China Earth Sciences, 56(12): 2045-2055.

Chen L. 2011. The metallogenesisof Oligocene Nuri skarn-porphyry Cu-W-Mo deposit in South Gangdese(doctoral dissertation)[D]. Supervisor: Qin K Z and Li G M. Beijing: Chinese Academy of Sciences(Institute of Geology and Geophysics). 91-100(in Chinese with English abstract).

Chen M H, Mo C S, Huang Z Z, Li B and Huang H W. 2011. Zircon LA-ICP-MS U-Pb ages of granitoid rocks and molybdenite Re-Os age of Shedong W-Mo deposit in Cangwu County of Guangxi and its geological significance[J]. Mineral Deposits, 30(6): 963-978(in Chinese with English abstract).

Chen X L, Liang H Y, Richards J P, Huang W T, Zhang J, Wu J and Sotiriou P. 2018. Age and granite association of skarn W mineralization at Niutangjie district, South China Block[J]. Ore Geology Reviews, 102: 268-283.

Chen Y X, Li H, Sun W D, Ireland T, Tian X F, Hu Y B, Yang W B, Chen C and Xu D R. 2016. Generation of Late Mesozoic Qianlishan A_2-type granite in Nanling Range, South China: Implications for Shizhuyuan W-Sn mineralization and tectonic evolution[J]. Lithos, 266: 435-452.

Chowdhury S and Lentz D R. 2011. Mineralogical and geochemical characteristics of scheelite-bearing skarns, and genetic relations between skarn mineralization and petrogenesis of the associated granitoid pluton at Sargipali, Sundergarh district, eastern India[J]. Journal of Geochemical Exploration, 108(1): 39-61.

Crowe D E, Riciput L R, Bezenek S and Ignatiev A. 2001. Oxygen isotope and trace element zoning in hydrothermal garnets: Windows into large-scale fluid-flow behavior[J]. Geology, 29(6): 479-482.

Dai P, Mao J, Wu S, Xie G and Luo X. 2018. Multiple dating and tectonic setting of the Early Cretaceous Xianglushan W deposit, Jiangxi Province, South China[J]. Ore Geology Reviews, 95: 1161-1178.

Deng X D, Li J W, Luo T and Wang H Q. 2017. Dating magmatic and hydrothermal processes using andradite-rich garnet U-Pb geochronometry[J]. Contributions to Mineralogy and Petrology, 172(9): 71.

Ding T, Ma D S, Lu J J and Zhang R Q. 2018. Garnet and scheelite as indicators of multi-stage tungsten mineralization in the Huangshaping deposit, southern Hunan Province, China[J]. Ore Geology Reviews, 94: 193-211.

Dong S H, Bi X W, Hu R Z and Chen Y W. 2014. Petrogenesis of Yaogangxian granites and implications for W mineralization, Hunan Province[J]. Acta Petrologica Sinica, 30(9): 2749-2765(in Chinese with English abstract).

Eichhorn R, Höll R, Jagoutz E and Schrer U. 1997. Dating scheelite stages: A strontium, neodymium, lead approach from the Felbertal tungsten deposit, Central Alps, Austria[J]. Geochimica et Cosmochimica Acta, 61: 5005-5022.

Fei X, Zhang Z, Cheng Z, Santosh M, Jin Z, Wen B, Li Z and Xu L. 2018. Highly differentiated magmas linked with polymetallic mineralization: A case study from the Cuihongshan granitic intrusions, Lesser Xing'an Range, NE China[J]. Lithos, 302: 158-177.

Feng C Y, Zeng Z L, Wang S, Liang J S and Ding M. 2012. SHRIMP zircon U-Pb and molybdenite Re-Os dating of the skarn-type tungsten deposits in southern Jiangxi Province, China, and geological implications: Examplified by the Jiaoli and Baoshan tungsten

polymetallic deposits[J]. Geotectonica at Metallogenia, 36(3): 337-349(in Chinese with English abstract).

Foster R P. 1977. Solubility of scheelite in hydrothermal chloride solutions[J]. Chemical Geology, 20(77): 27-43.

Gaspar M, Knaack C, Meinert L D and Moretti R. 2008. REE in skarn systems: A LA-ICP-MS study of garnets from the Crown Jewel gold deposit[J]. Geochimica et Cosmochimica Acta, 72(1): 185-205.

Ghaderi M, Palin J M, Campbell I H and Sylvester P J. 1999. Rare earth element systematics in scheelite from hydrothermal gold deposits in the Kalgoorlie-Norseman region, western Australia[J]. Econ. Geol., 94(3): 423-437.

Gibert F, Moine B, Schott J and Dan durand J L. 1992. Modeling of the transport and deposition of tungsten in the scheelite-bearing calc-silicate gneisses of the Montagne Noire, France[J]. Contributions to Mineralogy and Petrology, 112(2-3): 371-384.

Giuliani G, Cheilletz A and Mechiche M. 1987. Behaviour of REE during thermal metamorphism and hydrothermal infiltration associated with skarn and vein-type tungsten ore bodies in Central Morocco[J]. Chemical Geology, 64(3-4): 279-294.

Gleadow A J W and Lovering J F. 1978. Fission track geochronology of King Island, Bass Strait, Australia: Relationship to continental rifting[J]. Earth and Planetary Science Letters, 37(3): 429-437.

Graupner T, Kempe U, Dombon E, Pätzold O, Leeder O and Spooner E T C. 1999. Fluid regime and ore formation in the tungsten(-yttrium) deposits of Kyzyltau (Mongolian Altai): Evidence for fluid variability in tungsten-tin ore systems[J]. Chemical Geology, 154 (1-4): 21-58.

Guo C L, Chen Y C, Zeng Z L and Lou F S. 2012. Petrogenesis of the Xihuashan granites in southeastern China: Constraints from geochemistry and in-situ analyses of zircon U, Pb, Hf, O isotopes[J]. Lithos, 148(5Supp.): 209-227.

Guo Z J, Li J W, Xu X Y, Song Z Y, Dong X Z, Tian J, Yang Y C, She H Q, Xiang A P and Kang Y J. 2016. Sm-Nd dating and REE composition of scheelite for the Honghuaerji scheelite deposit, Inner Mongolia, northeast China[J]. Lithos, 261:307-321.

He X H and Gu S Y. 2017. Distribution characteristics of tungsten in the granite magma system and impact on mineralization[J]. Mineral Exploration, 8(4): 631-643(in Chinese with English abstract).

Heinrich C A, Günther D, Audétat A, Ulrich T and Frischknecht R. 1999. Metal fractionation between magmatic brine and vapor, determined by microanalysis of fluid inclusions[J]. Geology, 27(8): 755-758.

Higgins N C. 1980. Fluid inclusion evidence for the transport of tungsten by carbonate complexes in hydrothermal solutions[J]. Canadian Journal of Earth Sciences, 17(7): 823-830.

Huang W T, Wu J, Zhang J, Liang H Y and Qiu X L. 2017. Geochemistry and Hf-Nd isotope characteristics and forming processes of the Yuntoujie granites associated with W-Mo deposit, Guangxi, South China[J]. Ore Geology Reviews, 81: 953-964.

Hulsbosch N, Boiron M C, Dewaele S and Muchez P. 2016. Fluid fractionation of tungsten during granite-pegmatite differentiation and the metal source of peribatholitic W quartz veins: Evidence from the Karagwe-Ankole Belt (Rwanda)[J]. Geochimica et Cosmochimica Acta, 175(7): 299-318.

Hulsbosch N. 2019. Ore deposits: Origin, exploration, and exploitation[A]. In: DecréeS and Robb L, eds. Nb-Ta-Sn-W distribution in granite-related ore systems: Fractionation mechanisms and examples from the Karagwe-Ankole belt of Central Africa[C]. New York: John Wiley and Sons, 242: 75-107.

Ishihara S, Wang P A, Kajiwara Y and Watanabe Y. 2003. Origin of sulfur in some magmatic-hydrothermal ore deposits of South China[J]. Bulletin of Geological Survey of Japan, 54(3/4): 161-169.

Ismail R, Ciobanu C L, Cook N J, Teale G S, Giles D, Mumm A S and Wade B. 2014. Rare earths and other trace elements in minerals from skarn assemblages, Hillside iron oxide-copper-gold deposit, Yorke Peninsula, South Australia[J]. Lithos, 184: 456-477.

Jiang S H, Bagas L, Hu P, Han N, Chen C L and Liu Y. 2016. Zircon U-Pb ages and Sr-Nd-Hf isotopes of the highly fractionated granite with tetrad REE patterns in the Shamai tungsten deposit in eastern Inner Mongolia, China: Implications for the timing of mineralization and ore genesis[J]. Lithos, 261: 322-339.

Kang Y F and Li C Y. 1991. Geological characteristics, types and distribution of tungsten deposits in China[J]. Mineral Deposits, 10(1): 19-26(in Chinese with English abstract).

Kempe U, Belyatsky B, Krymsky R, Kremenetsky A and Ivanov P. 2001. Sm-Nd and Sr isotope systematics of scheelite from the giant Au(-W) deposit Muruntau (Uzbekistan): Implications for the age and sources of Au mineralization[J]. Mineralium Deposita, 36 (5): 379-392.

Keppler H and Wyllie P J. 1991. Partitioning of Cu, Sn, Mo, W, U, and Th between melt and aqueous fluid in the systems haplogranite-H_2O-HCl and haplogranite-H_2O-HF[J]. Contributions to Mineralogy and Petrology, 109(2): 139-150.

Korges M, Weis P, Lüders V and Laurent O. 2017. Depressurization and boiling of a single magmatic fluid as a mechanism for tin-tungsten deposit formation[J]. Geology, 46(1): 75-78.

Kozlik M, Gerdes A and Raith J G. 2016. Strontium isotope systematics of scheelite and apatite from the Felbertal tungsten deposit, Austria-Results of in-situ LA-MC-ICP-MS analysis[J]. Mineralogy and Petrology, 110(1): 11-27.

Kwak T A P and Tan T H. 1981. The geochemistry of zoning in skarn minerals atthe King Island (Dolphin) mine[J]. Econ. Geol., 76: 468-497.

Lecumberri-Sanchez P, Vieira R, Heinrich C A, Pinto F and Wälle M. 2017. Fluid-rock interaction is decisive for the formation of tungsten deposits[J]. Geology, 45(7): 579-582.

Li X F, Feng Z H, Xiao R, Song C A, Yang F, Wang C Y, Kang Z Q and Mao W. 2012. Spatial and temporal distributions and the geological setting of the W-Sn-Mo-Nb-Ta deposits at the northeastern Guangxi, South China[J]. Acta Geologica Sinica, 86(11): 1713-1725(in Chinese with English abstract).

Li X F, Huang C, Wang C Z and Wang L F. 2016. Genesis of the Huangshaping W-Mo-Cu-Pb-Zn polymetallic deposit in southeastern Hunan Province, China: Constraints from fluid inclusions, trace elements, and isotopes[J]. Ore Geology Reviews, 79: 1-25.

Li X F, Yu Y and Wang C Z. 2017. Caledonian granitoids in the Jinxiu area, Guangxi, South China: Implications for their tectonic setting[J]. Lithos, 272: 249-260.

Li X H, Li W X and Li Z X. 2007. On the genetic classification and tectonic implications of the Early Yanshanian granitoids in the Nanling Range, South China[J]. Chinese Science Bulletin, 52(9): 981-991(in Chinese).

Li Y F, Mao J W, Bai F J, Li J P and He Z J. 2003. Re-Os isotopic dating of molybdenite in the Nannihumolybdenum(tungsten) orefield in the eastern Qinling and its geological significance[J]. Geological Review, 49(6): 652-659(in Chinese with English abstract).

Li Y, Yu X, Mi K, Carranza EJM, Liu J, Jia W and He S. 2019. Deposit geology, geochronology and geochemistry of the Gongpengzi skarn Cu-Zn-W polymetallic deposit, NE China[J]. Ore Geology Reviews, 109: 465-481.

Lin S P. 2016. Magmatism and mineralization in the Miaoershan-Yuechenglingorefield of NE Guangxi(doctoral dissertation) [D]. Supervisor: Liang H Y. Guangzhou: Chinese Academy of Sciences (Guangzhou Institute of Geochemistry). 60p(in Chinese with English abstract).

Lin Y H. 1982. Types and geological characteristics of scheelite deposits[J]. Geology and Exploration, (6): 15-23.

Linnen R L and Williams-Jones A E. 1994. The evolution of pegmatite-hosted Sn-W mineralization at NongSua, Thailand: Evidence from fluid inclusions and stable isotopes[J]. Geochimica et Cosmochimica Acta, 58(2):735-747.

Linnen R L and Cuney M. 2005. Granite-related rare-element deposits and experimental constraints on Ta-Nb-W-Sn-Zr-Hf mineralization[J]. Journal of Post Keynesian Economics, 1(1): 6-15.

Liu Y, Deng J, Li C F, Shi G H and Zheng A L. 2007. REE composition in scheelite and scheelite Sm-Nd dating for the Xuebao-ding W-Sn-Be deposit in Sichuan[J]. Chinese Science Bulletin, 52(18): 2543-2550.

Lowenstern J B. 2001. Carbon dioxide in magmas and implications for hydrothermal systems[J]. Mineralium Deposita, 36(6): 490-502.

Lu H Z, Liu Y M, Wang C L, Xu Y Z and Li H Q. 2003. Mineralization and fluid inclusion study of the Shizhuyuan W-Sn-Bi-Mo-F skarn deposit, Hunan Province, China[J]. Econ. Geol., 98(5): 955-974.

Manning D A C and Henderson P. 1984. The behaviour of tungsten in granitic melt-vapour systems[J]. Contributions to Mineralogy and Petrology, 86(3): 286-293.

Mao B, Ye H S, Li C, Wang Z M, Yan G L, Gao Y and Xiong B K. 2010. Geological characteristics and Re-Os isotopic age of Yechangping porphyry-skarn type Mo deposit in western Henan[J]. Mineral Deposits, 29(Supp.1): 493-494(in Chinese).

Mao J W, Xiong B, Liu J, Pirajno F, Cheng Y B, Ye H S, Song S W and Dai P. 2017. Molybdenite Re/Os dating, zircon U-Pb age and geochemistry of granitoids in the Yangchuling porphyry W-Mo deposit (Jiangnan tungsten ore belt), China: Implications for petrogenesis, mineralization and geodynamic setting[J]. Lithos, 286: 35-52.

Mathieson G A and Clark A H. 1984. The Cantung E Zone scheelite skarn orebody, Tungsten, northwest Territories: A revised genetic model[J]. Econ. Geol., 79(5): 883-901.

Meinert L D, Hedenquist J W, Satoh H and Matsuhisa Y. 2003. Formation of anhydrous and hydrous skarn in Cu-Au ore deposits by magmatic fluids[J]. Econ. Geol., 98(1): 147-156.

Meinert L D, Dipple G M and Nicolescu S. 2005. World skarn deposits[J]. Econ. Geol., 100: 299-336.

Mueller A G, de Laeter J R and Groves D I. 1991. Strontium isotope systematics of hydrothermal minerals from epigenetic Archean gold deposits in the Yilgarn Block, western Australia[J]. Econ. Geol., 86(4): 780-809.

Newberry R J and Einaudi M T. 1981. Tectonic and geochemical setting of tungsten skarn mineralization in the Cordillera[M]. Arizona Geological Society Digest, 14: 99-111.

Newberry R J and Swanson S E. 1986. Scheelite skarn granitoids: An evaluation of the roles of magmatic source and process[J]. Ore Geology Reviews, 1(1): 57-81.

Newberry R J. 1983. The formation of subcalcic garnet in scheelite-bearing skarns[J]. Canadian Mineralogist, 21: 529-544.

Ni P, Wang X D, Wang G G, Huang J B, Pan J Y and Wang T G. 2015. An infrared microthermometric study of fluid inclusions in coexisting quartz and wolframite from Late Mesozoic tungsten deposits in the Gannanmetallogenic belt, South China[J]. Ore Geology Reviews, 65: 1062-1077.

O'reilly C, Gallagher V and Feely M. 1997. Fluid inclusion study of the Ballinglen W-Sn-sulphide mineralization, SE Ireland[J]. Mineralium Deposita, 32(6): 569-580.

Orhan A. 2017. Evolution of the Mo-rich scheelite skarn mineralization at Kozbudaklar, western Anatolia, Turkey: Evidence from mineral chemistry and fluid inclusions[J]. Ore Geology Reviews, 80: 141-165.

Pan X F, Hou Z Q, Li Y, Chen G H, Zhao M, Zhang T F, Zhang C, Wei J and Kang C. 2017. Dating the giant Zhuxi W-Cu deposit (Taqian-Fuchun Ore Belt) in South China using molybdenite Re-Os and muscovite Ar-Ar system[J]. Ore Geology Reviews, 86: 719-733.

Park C, Song Y, Kang I M, Shim J, Chung D and Park C S. 2017. Metasomatic changes during periodic fluid flux recorded in grandite garnet from the Weondong W-skarn deposit, South Korea[J]. Chemical Geology, 451: 135-153.

Peng B and Frei R. 2004. Nd-Sr-Pb isotopic constraints on metal and fluid sources in W-Sb-Au mineralization at Woxi and Liaojiaping (western Hunan, China)[J]. Mineralium Deposita, 39: 313-327.

Peng J T, Zhou M F, Hu R Z, Shen N P, Yuan S D, Bi X W, Du A D and Qu W J. 2006. Precise molybdenite Re-Os and mica Ar-Ar dating of the Mesozoic Yaogangxian tungsten deposit, Central Nanling district, South China[J]. Mineralium Deposita, 41(7): 661-669.

Poulin R S, Kontak D J, McDonald A and McClenaghan M B. 2018. Assessing scheelite as an ore-deposit discriminator using its trace-element and REE chemistry[J]. Canadian Mineralogist, 56(3): 26-302.

Qin Y, Wang D H, Li Y H, Wang K Y, Wu L B and Mei Y P. 2010. Rock-forming and ore-forming ages of the Baizhangyan tungsten-molybdenum ore deposit in Qingyang, Anhui Province and their geological significance[J]. Earth Science Frontiers, 17(2): 170-177 (in Chinese with English abstract).

Rasmussen K L, Lentz D R, Falck H and Pattison D R M. 2011. Felsic magmatic phases and the role of late-stage aplitic dykes in the formation of the world-class Cantung Tungsten skarn deposit, northwest Territories, Canada[J]. Ore Geology Reviews, 41(1): 75-111.

Roberts S, Palmer M R and Waller L. 2006. Sm-Nd and REE characteristics of tourmaline and scheelite from the Bjorkdal gold deposit, northern Sweden: Evidence of an intrusion-related gold deposit[J]? Econ. Geol., 101(7): 1415-1425.

Romer R L and Kroner U. 2014. Sediment andweathering control on the distribution of Paleozoic magmatic tin-tungsten mineralization[J]. Mineralium Deposita 50: 327-338.

Romer R L and Kroner U. 2016. Phanerozoic tin and tungsten mineralization-Tectonic controls on the distribution of enriched protoliths and heat sources for crustal melting[J]. Gondwana Research, 31: 60-95.

Rudnick R L and Gao S. 2003. The Crust[A]. In: Rudnick R L, ed. Composition of the Continental Crust[C]. Oxford: Elsevier-Pergamon. 1-64.

Sánchez S M T, Benito M C M and Pérez M L C. 2009. Mineralogical and physiochemical evolution of the Los Santos scheelite skarn, Salamanca, NW Spain[J]. Econ. Geol., 104(7): 961-995.

Scanlan E J, Scott J M, Wilson V J, Stirling C H, Reid M R and Le Roux P J. 2018. In situ $^{87}Sr/^{86}Sr$ of scheelite and calcite reveals proximal and distal fluid-Rock interaction during orogenic W-Au mineralization, Otago Schist, New Zealand[J]. Econ. Geol., 113 (7): 1571-1586.

Selby D, Creaser R A, Heaman L M and Hart C J R. 2003. Re-Os and U-Pb geochronology of the Clear Creek, Dublin Gulch, and Mactung deposits, Tombstone gold belt, Yukon, Canada: Absolute timing relationships between plutonism and mineralization[J]. Canadian Journal of Earth Sciences, 40(12): 1839-1852.

Seman S, Stockli D F and Mclean N M. 2017. U-Pb geochronology of grossular-andradite garnet[J]. Chemical Geology, 460: 106-116.

Seo J H, Yoo B C, Villa I M, Lee J H, Kim C and Moon K J. 2017. Magmatic-Hydrothermal Processes in Sangdong W-Mo deposit, Korea: Study of fluid inclusions and ^{39}Ar-^{40}Ar geochronology[J]. Ore Geology Reviews, 91: 316-334.

Shelton K L, Taylor R P and So C S. 1987. Stable isotope studies of the Dae Hwa tungsten-molybdenum mine, Republic of Korea; evidence of progressive meteoric water interaction in a tungsten-bearing hydrothermal system[J]. Econ. Geol., 82(2): 471-481.

Sheng J F, Liu L J, Wang D H, Cheng Z H, Ying L J, Huang F, Wang J H and Zeng L. 2015. A preliminary review of metallogenicregularity of tungsten deposits in China[J]. Acta Geologica Sinica (English Edition), 89(4): 1359-1374.

Shi H S, Lin F C and Zhang L K. 2009. Spatio-temporaldistribution and current state ofthe research of the tungsten deposits: An overview[J]. Sedimentary Geology and Tethyan Geology, 29(4): 90-95 (in Chinese with English abstract).

Singoyi B and Zaw K. 2001. A petrological and fluid inclusion study of magnetite-scheelite skarn mineralization at Kara, northwestern Tasmania: Implications for ore genesis[J]. Chemical Geology, 173 (1): 239-253.

Skaarup P. 1974. Strata-bound scheelite mineralisation in skarns and gneisses from the Bindal area, northern Norway[J]. Mineralium Deposita, 9(4): 299-308.

Smith M P, Henderson P, Jeffries T E R, Long J and Williams C T. 2004. The rare earth elements and uranium in garnets from the Beinn an Dubhaich Aureole, Skye, Scotland, UK: Constraints on processes in a dynamic hydrothermal system[J]. Journal of Petrology, 45(3): 457-484.

Soloviev S G, Kryazhev S G and Dvurechenskaya S S. 2017. Geology, mineralization, stable isotope, and fluid inclusion characteristics of the Vostok-2 reduced W-Cu skarn and Au-W-Bi-As stockwork deposit, Sikhote-Alin, Russia[J]. Ore Geology Reviews, 86: 338-365.

Song G X, Qi K Z, Li G M, Evans N J and Chen L. 2014. Scheelite elemental and isotopic signatures: Implications for the genesis of skarn-type W-Mo deposits in the Chizhouarea, Anhui Province, eastern China[J]. American Mineralogist, 99: 303-317.

Song G X, Cook N J, Li G M, Qin K Z, Ciobanu C L, Yang Y H and Xu Y X. 2019. Scheelite geochemistry in porphyry-skarn W-Mo systems: A case study from the Gaojiabangdeposit, East China[J]. Ore Geology Reviews, 113: 103084.

Song S W, Mao J W, Xie G Q, Chen L, Santosh M, Chen G H, Rao J F and Ouyang Y P. 2018. In situ LA-ICP-MS U-Pb geochronology and trace element analysis of hydrothermal titanite from the giant Zhuxi W (Cu) skarn deposit, South China[J]. Mineralium Deposita, 54:569-590.

Sugaki A, Kusachi I and Shimada N. 1988. Granite-series and types of igneous rocks in the Bolivian Andes and their genetic relation to tin-tungsten mineralization[J]. Mining Geology, 38(208): 121-130.

Sun K K and Chen B. 2017. Trace elements and Sr-Nd isotopes of scheelite: Implications for the W-Cu-Mo polymetallic mineralization of the Shimensi deposit, South China[J]. American Mineralogist, 102(5): 1114-1128.

Sun K K, Chen B and Deng J. 2019. Ore genesis of the Zhuxi supergiant W-Cu skarn polymetallic deposit, South China: Evidence from scheelite geochemistry[J]. Ore Geology Reviews, 107: 14-29.

Taylor J R and Wall V J. 1992. The behaviour of tin in granitoid magmas[J]. Econ. Geol., 87: 403-420.

Tornos F, Galindo C, Crespo J L and Spiro B F. 2008. Geochemistry and origin of calcic tungsten-bearing skarns, Los Santos (Central

Iberian Zone, Spain)[J]. Canadian Mineralogist, 46(1): 87-109.

Voicu G, Bardoux M, Stevenson R and Jebrak M. 2000. Nd and Sr isotope study of hydrothermal scheelite and host rocks at Omai, Guiana Shield: Implications for ore fluid source and flow path during the formation of orogenic gold deposits[J]. Mineralium Deposita, 35(4): 302-314.

Wang Y Y, Kerkhof A V D, Xiao Y L, Sun H, Yang X Y, Lai J Q and Wang Y G. 2017. Geochemistry and fluid inclusions of scheelite-mineralized granodiorite porphyries from southern Anhui Province, China[J]. Ore Geology Reviews, 89: 988-1005

Wei W F, Hu R Z, Bi X W, Peng J T, Su W C, Song S Q and Shi S H. 2012. Infrared microthermometric and stable isotopic study of fluid inclusions in wolframite at the Xihuashan tungsten deposit, Jiangxi Province, China[J]. Mineralium Deposita, 47(6): 589-605.

Wintzer N E, Gillerman V S and Schmitz M D. 2016. Eocene U-Pb scheelite LA-ICP-MS dates of stibnite-scheelite mineralization in the yellow pine Au-Sb-W mining area, Central Idaho, USA[C]. GSA Meeting in Denver, Colorado, USA.

Wood S A and Samson I M. 2000. The hydrothermal geochemistry of tungsten in granitoid environments: I. Relative solubilities of ferberite and scheelite as a function of T, P, pH, and m_{NaCl}[J]. Econ. Geol., 95(1): 143-182.

Wu F Y, Liu X C, Ji W Q, Wang J M and Yang L. 2017. Highly fractionated granites: Recognition and research[J]. Science China Earth Sciences, 47(7): 745-765(in Chinese).

Xia Q L, Wang X Q, Liu Z Z, Li T F and Feng L. 2018. Tungsten metallogenic and geological features and mineral resource potential in China[J]. Earth Science Frontiers, 2018, 25(3): 50-58. (in Chinese with English abstract).

Xiao X, Zhou T F, Yuan F, Fan Y, Zhang D Y, Liu D Z, Huang W P and Chen X F. 2017. The geochronology of the QingyangGaojiabang tungsten-molybdenum deposit and its geological significance, Anhui Province, East China[J]. Act Petrologica Sinica, 33(3): 859-872(in Chinese with English abstract).

Xie G Q, Mao J W, Li W, Fu B and Zhang Z Y. 2018. Granite-related Yangjiashan tungsten deposit, southern China[J]. Mineralium Deposita, 54(1): 67-80.

Xu J, Ciobanu C L, Cook N J, Zheng Y Y, Sun X and Wade B P. 2016. Alteration and mineralization at the Zhibula Cu skarn deposit, Gangdese belt, Tibet[J]. Ore Geology Reviews, 75: 304-326.

Xu J, Ciobanu C L, Cook N J and Slaterry A. 2019. Crystals from the scheelite-powellite solid-solution series at the nanoscale: The Zhibula Cu skarn, Gangdesebelt, Tibet[J].Minerals, 9(6): 340.

Xu K Q and Chen H. 1987. Tectonic setting of tungsten deposit in China[J]. Contributions to Geology and Mineral Resources Research, 2(3): 1-7(in Chinese).

Yu Q, Chen G H and Kang C. 2018. Study of metallogenic chronology, mineralogy and ore-forming process of the superlarge tungsten deposits in Zhuxi, Jiangxi Province[J]. Geological Journal of China Universities, 24(6): 880-111(in Chinese with English abstract).

Yuan S D, Zhang D L, Shuang Y, Du A D and Qu W J. 2012. Re-Os dating of molybdenite from the Xintianling giant tungsten-molybdenite deposit in southern Hunan Province, China and its geological implications[J]. Acta Petrological Sinica, 28(1): 29-40(in Chinese with English abstract).

Zajacz Z, Halter W E, Pettke T and Guillong M. 2008. Determination of fluid/melt partition coefficients by LA-ICP-MS analysis of coexisting fluid and silicate melt inclusions: Controls on element partitioning[J]. Geochimica et Cosmochimica Acta, 72(8): 2169-2197.

Zaw K and Singoyi B. 2000. Formation of magnetite-scheelite skarn mineralization at Kara, northwestern Tasmania: Evidence from mineral chemistry and stable isotopes[J]. Econ. Geol., 95(6): 1215-1230.

Zhai D G, Liu J J, Zhang H Y, Wang J P, Su L, Yang X A and Wu S H. 2014. Origin of oscillatory zoned garnets from the Xieertala Fe-Zn skarn deposit, northern China: In situ, LA-ICP-MS evidence[J]. Lithos, 190-191(2): 279-291.

Zhang Y, Zhang S, Tan S, Cui Y, Zhao Z, Jiang Y, Jiang S and Tao S. 2016. The genetic relationship between the large Guanfang W deposit and granitic intrusions, in Yunnan Province, southwest China: Evidence from U-Pb and Re-Os geochronology and Pb and Sr isotopic characteristics[J]. Ore Geology Reviews, 79: 332-345.

Zhang Y, Yang J H, Chen J Y, Wang H and Xiang Y X. 2017. Petrogenesis of Jurassic tungsten-bearing granites in the Nanling Range, South China: Evidence from whole-rock geochemistry and zircon U-Pb and Hf-O isotopes[J]. Lithos, 278-281: 166-180.

Zhao B and Barton M D. 1987. Compositional characteristics of garnets and pyroxenes in contact-metasomatic skarn deposits and their relationship to mineralization[J]. Acta MineralogicaSinica, 7 (1): 4-11(in Chinese with English abstract).

Zhao P, Yuan S, Mao J, Santosh M, Li C and Hou K. 2016. Geochronological and petrogeochemical constraints on the skarn deposits in Tongshanling ore district, southern Hunan Province: Implications for Jurassic Cu and W metallogenic events in South China[J]. Ore Geology Reviews, 78: 120-137.

Zhao W W, Zhou M F, Williams-Jones A E and Zhao Z. 2017. Constraints on the uptake of REE by scheelite in the Baoshan tungsten skarn deposit, South China[J]. Chemical Geology, 477: 123-136.

Zhao W W and Zhou M F. 2018. Mineralogical and metasomatic evolution of the Jurassic Baoshan scheelite skarn deposit, Nanling, South China[J]. Ore Geology Reviews, 95: 182-194.

Zheng Y, Ding Z, Cawood P A and Yue S. 2017. Geology, geochronology and isotopic geochemistry of the Xiaoliugou W-Mo ore field in the Qilian orogen, NW China: Case study of a skarn system formed during continental collision[J]. Ore Geology Reviews, 81: 575-586.

Zhou J H, Feng C Y, Li D X and Li G C. 2016a. Geological, geochemical, and geochronological characteristics of Caledonian W-Sn mineralization in the Baiganhuorefield, southeastern Xinjiang, China[J]. Ore Geology Reviews, 75: 125-149.

Zhou J H, Feng C Yand Li D X. 2016b. Geochemistry of the garnets in

the Baiganhu W-Sn orefield, NW China[J]. Ore Geology Reviews, 82: 70-92.

Zhou X M, Sun T, Shen W Z, Shu L S and Niu Y L. 2006. Petrogenesis of Mesozoic granitoids and volcanic rocks in South China: A response to tectonic evolution[J]. Episodes, 29(1): 26.

Zhou Y, Liang X Q, Wu S C, Cai Y F, Liang X R, Shao T B, Ce W, Fu J G and Ying J. 2015. Isotopic geochemistry, zircon U-Pb ages and Hf isotopes of A-type granites from the Xitian W-Sn deposit, SE China: Constraints on petrogenesis and tectonic significance[J]. Journal of Asian Earth Sciences, 105(6): 122-139.

附中文参考文献

毕承思. 1987. 中国矽卡岩型白钨矿矿床成矿基本地质特征[J]. 中国地质科学院院报,17(3): 49-64.

蔡明海,韩凤彬,何龙清,刘国庆,陈开旭,付建明. 2008. 湘南新田岭白钨矿床 He-Ar 同位素特征及 Rb-Sr 测年[J]. 地球学报,29(2): 167-173.

陈雷. 2011. 冈底斯南缘渐新世努日矽卡岩-斑岩型铜钨钼矿床成矿作用研究(博士论文)[D]. 导师:秦克章,李光明.北京: 中国科学院研究生院(地质与地球物理研究所).91-100 页.

陈懋弘,莫次生,黄智忠,李斌,黄宏伟. 2011. 广西苍梧县社洞钨钼矿床花岗岩类锆石 LA-ICP-MS 和辉钼矿 Re-Os 年龄及其地质意义[J]. 矿床地质,30(6):963-978.

董少花,毕献武,胡瑞忠,陈佑纬.2014. 湖南瑶岗仙复式花岗岩岩石成因及与钨成矿关系[J]. 岩石学报,30(9): 2749-2765.

丰成友,曾载淋,王松,梁景时,丁明.2012. 赣南矽卡岩型钨矿成岩成矿年代学及地质意义——以焦里和宝山矿床为例[J]. 大地构造与成矿学,36(3): 337-349.

何兴华,顾尚义. 2017. 钨在花岗岩岩浆体系中的分配特征以及对成矿作用的影响[J]. 矿产勘查,8(4): 631-643.

康永孚,李崇佑. 1991. 中国钨矿床地质特征、类型及其分布[J]. 矿床地质,10(1): 19-26.

李献华,李武显,李正祥. 2007. 再论南岭燕山早期花岗岩的成因类型与构造意义[J]. 科学通报,52(9): 981-991.

李晓峰,冯佐海,肖荣,宋慈安,杨锋,王翠云,康志强,毛伟. 2012. 桂东北钨锡稀有金属矿床的成矿类型,成矿时代及其地质背景[J]. 地质学报,86(11): 1713-1725.

李永峰,毛景文,白凤军,李俊平,何志军.2003. 东秦岭南泥湖钼(钨)矿田 Re-Os 同位素年龄及其地质意义[J]. 地质论评,49(6):652-659.

林书平. 2016. 桂东北苗儿山—越城岭矿集区成岩成矿演化分析(博士论文)[D]. 导师:梁华英.广州:中国科学院研究生院(广州地球化学研究所). 60 页.

林运淮. 1982. 白钨矿矿床类型及其地质特征[J]. 地质与勘探,6:15-23.

毛冰,叶会寿,李超,王佐满,晏国龙,高阳,熊必康. 2010. 豫西夜长坪斑岩-矽卡岩型钼矿床地质特征及其辉钼矿铼-锇同位素年龄[J]. 矿床地质,29(S1): 493-494.

秦燕,王登红,李延河,王克友,吴礼彬,梅玉萍. 2010. 安徽青阳百丈岩钨钼矿床成岩成矿年龄测定及地质意义[J]. 地学前缘,17(2): 170-177.

石洪召,林方成,张林奎. 2009. 钨矿床的时空分布及研究现状[J]. 沉积与特提斯地质,29(4): 90-95.

吴福元,刘小驰,纪伟强,王佳敏,杨雷. 2017. 高分异花岗岩的识别与研究[J]. 中国科学:地球科学,47(7): 745-765.

夏庆霖,汪新庆,刘壮壮,李童斐,冯磊. 2018. 中国钨矿成矿地质特征与资源潜力分析[J]. 地学前缘,25(3): 50-58.

肖鑫,周涛发,袁峰,范羽,张达玉,刘东周,黄伟平,陈雪锋. 2017. 安徽青阳高家塝钨钼矿床成岩成矿时代及其地质意义[J]. 岩石学报,33(3): 859-872.

徐克勤,程海. 1987. 中国钨矿形成的大地构造背景[J]. 地质找矿论丛,2(3): 1-7.

于全,陈国华,康川. 2018. 江西朱溪超大型钨矿床成矿年代学、矿物学及成矿过程研究[J]. 高校地质学报,24(6):88-111.

袁顺达,张东亮,双燕,杜安道,屈文俊. 2012. 湘南新田岭大型钨钼矿床辉钼矿 Re-Os 同位素测年及其地质意义[J]. 岩石学报,28(1): 29-40.

赵斌,Barton M D. 1987. 接触交代夕卡岩型矿床中石榴子石和辉石成分特点及其与矿化的关系[J]. 矿物学报,(7)1: 4-11.